Journal of Cerebral Blood Flow & Metabolism (2015) 35, 1836–1845

www.jcbfm.com

ORIGINAL ARTICLE

Selective neuronal vulnerability of human hippocampal CA1 neurons: lesion evolution, temporal course, and pattern of hippocampal damage in diffusion-weighted MR imaging

Thorsten Bartsch[1], Juliane Döhring[1], Sigrid Reuter[1], Carsten Finke[2], Axel Rohr[3], Henriette Brauer[1], Günther Deuschl[1] and Olav Jansen[3]

The CA1 (cornu ammonis) region of hippocampus is selectively vulnerable to a variety of metabolic and cytotoxic insults, which is mirrored in a delayed neuronal death of CA1 neurons. The basis and mechanisms of this regional susceptibility of CA1 neurons are poorly understood, and the correlates in human diseases affecting the hippocampus are not clear. Adopting a translational approach, the lesion evolution, temporal course, pattern of diffusion changes, and damage in hippocampal CA1 in acute neurologic disorders were studied using high-resolution magnetic resonance imaging. In patients with hippocampal ischemia ($n = 50$), limbic encephalitis ($n = 30$), after status epilepticus ($n = 17$), and transient global amnesia ($n = 53$), the CA1 region was selectively affected compared with other CA regions of the hippocampus. CA1 neurons exhibited a maximum decrease of apparent diffusion coefficient (ADC) 48 to 72 hours after the insult, irrespective of the nature of the insult. Hypoxic-ischemic insults led to a significant lower ADC suggesting that the ischemic insult results in a stronger impairment of cellular metabolism. The evolution of diffusion changes show that CA1 diffusion lesions mirror the delayed time course of the pathophysiologic cascade typically observed in animal models. Studying the imaging correlates of hippocampal damage in humans provides valuable insight into the pathophysiology and neurobiology of the hippocampus.

Journal of Cerebral Blood Flow & Metabolism (2015) **35,** 1836–1845; doi:10.1038/jcbfm.2015.137; published online 17 June 2015

Keywords: CA1; encephalitis; hippocampus; memory; stroke; vulnerability

INTRODUCTION

For over 130 years, it has been known that pathologic insults, such as ischemia, hypoglycemia, oxidative stress, and anoxia, can cause structural damage to the hippocampus. The hippocampus responds to these pathologic conditions with a heterogeneous susceptibility as the cellular damage is most clearly displayed in the CA1 (cornu ammonis) subfield.[1,2] The vulnerability of the CA1 region was initially studied after transient ischemia in the gerbil[3] and rat[4] showing a time course with a 'delayed neuronal death' of CA1 neurons 48 to 72 hours after reperfusion whereas the dentate gyrus, CA3, and most cortical neurons appear to be more resistant. In primate models, neuronal damage occurring after ischemia depends on the magnitude of the insult; ischemia in monkeys for up to 5 minutes results in almost no damage, whereas 10 to 15 minutes of ischemia leads to the selective degeneration of CA1 pyramidal cells. A longer duration of ischemia results in damage to structures outside of the hippocampus, such as neocortical layers III, V, and VI, and the striatum.

Although the cellular cascade leading from initial hit to subsequent damage and degeneration has been characterized in the past decades, the exact mechanisms of this region-specific selective vulnerability are not well understood but may include genomic-dependent glutamate- and calcium-mediated mechanisms of neuronal excitotoxicity and oxidative stress as well as inflammatory changes.[5]

In humans, the hippocampus can be affected by various insults such as ischemia, inflammation, hypoglycemia, or excessive metabolic demand during epileptic activity that may result in impairment of functional and structural neuronal integrity. As hippocampal circuits, in particular CA1 circuits, are critically involved in the process of memory formation and consolidation,[6] an affection of CA1 neurons prominently contributes to memory impairment and neurologic disability seen in patients during the course of diseases damaging the hippocampus and represent a large part of the chronic disease burden.[7]

Restriction of water diffusion linked to impairment of cellular metabolism or perfusion and damage in the hippocampus can be noninvasively detected using diffusion-weighted magnetic resonance imaging (DW–MRI).[8,9] Neuronal damages result in the breakdown of energy-dependent Na/K-ATPases with subsequent cellular swelling and cytotoxic edema. The metabolic changes that occur during the course of various pathologic processes result in a reduced net diffusion of water molecules by Brownian motion, which can be measured as a reduction in the apparent diffusion coefficient (ADC) using MRI.[10] Thus, the ADC reflects the degree of abnormal water movement in injured tissue that can be caused by

[1]Department of Neurology, Memory Disorders and Plasticity Group, University Hospital Schleswig-Holstein, Kiel, Germany; [2]Department of Neurology, Charité Universitätsmedizin Berlin, Berlin, Germany and [3]Institute of Neuroradiology, University Hospital Schleswig-Holstein, Kiel, Germany. Correspondence: Professor T Bartsch, Department of Neurology, Memory Disorders and Plasticity Group, University Hospital Schleswig-Holstein, Schittenhelmstr. 10, Kiel 24105, Germany.
E-mail: t.bartsch@neurologie.uni-kiel.de
This study was supported by Deutsche Forschungsgemeinschaft SFB 654 (TP A14; to TB), EXC 306 Inflammation at Interfaces, and by the Faculty of Medicine, University of Kiel, Germany.
Received 12 January 2015; revised 5 May 2015; accepted 18 May 2015; published online 17 June 2015

a net shift of water from the extracellular to intracellular compartments and by a reduced transmembrane permeability caused by the collapse of energy-dependent transmembrane ion gradients. Although DW–MRI does not detect cellular metabolic derangements or derangements of perfusion *per se*, it is hence a sensitive tool for indirectly and nonspecifically detecting severe metabolic changes during neuropathologic states that result in cytotoxic edema and abnormal Brownian motion of water molecules. Indeed, global changes of the ADC in the hippocampus have been observed in hippocampal stroke,[11] herpes simplex encephalitis (HSE),[12] limbic encephalitis (LE),[13] status epilepticus,[14] and transient global amnesia (TGA),[15] but the evolution of lesions, spatial pattern, and time course of damage to CA1 in etiologically different neurologic diseases is elusive.

Thus, considering the characteristic pathophysiologic consequences of insult to hippocampal neurons in animals, the aim of the study was to gain a translational insight into the differential response pattern of human CA1 neurons to various insults. We hence studied and compared the quantitative, temporal, and spatial characteristics of diffusion changes in the CA1 region in patients with acute ischemia, encephalitis, epilepsy, and TGA. Some of the results have been published in abstract form.[16]

PATIENTS AND METHODS

Patient Cohorts

Imaging and clinical data were retrospectively studied on patients admitted to our department between 2000 and 2011 presenting with acute memory deficits, seizures, or neurologic symptoms suggestive for an ischemic stroke, encephalitis, status epilepticus, or TGA, and in which MRI showed an affection of the hippocampus. Also, an extensive and careful review of hospital records was undertaken to retrospectively identify patients with the aforementioned disorders showing an affection of the hippocampus. Patients had a standard clinical neurologic examination on admission, and the history of vascular and nonvascular risk factors including a history of neurologic diseases was taken (Table 1). The high number of patients seen reflects a regional stroke awareness program with very early admittance of large numbers of patients with suspected stroke. The study was approved by the Ethical Committee of the University of Kiel and was conducted according to the Declaration of Helsinki.

Hippocampal ischemia. Fifty patients (35 men and 15 women, mean age 64.2 ± 15 years) were studied presenting with an acute ischemia in the posterior circulation involving the hippocampus or the territory of the anterior choroidal artery.

Status epilepticus. Seventeen patients (6 men and 11 women, mean age 59.1 ± 22 years) were studied presenting with a status epilepticus or a series of seizures characterized by continuous convulsive and nonconvulsive seizures lasting longer than 5 minutes or two or more seizures during which the patient did not return to baseline consciousness according to the criteria of the International League Against Epilepsy. The cohort of seizure patients was pooled with regard to the different etiologies of the seizure: diabetes mellitus type 1 with or without hypoglycemia ($n = 3$), cortical dysplasia, HIV leukoencephalopathy, *de novo* status epilepticus of unknown origin ($n = 4$), brain tumor or filiae ($n = 4$), and symptomatic epilepsy after stroke ($n = 6$).

Acute encephalitis. We studied 30 patients (17 men and 13 women, mean age 60.9 ± 17 years) presenting with either a viral or nonviral LE and evidence of an affection of the hippocampus on MRI or additional affection of other limbic/temporomesial structures typical for LE.[13] The clinical symptoms included subacute temporal lobe seizures, alteration of consciousness, memory disturbances, and focal neurologic deficits that were accompanied by various neuropsychiatric symptoms, such as disorientation, confusion, and behavioral abnormalities. Considering the frequent prodromal disease phase for the temporal analysis, the first observed clinical symptoms were taken as disease onset. Diagnostic criteria for viral encephalitis relied on detection of either Herpes simplex virus (HSV) DNA in the cerebrospinal fluid (CSF), positive antibody assay for neurotropic agents, or typical inflammatory CSF constellation.

Limbic encephalitis was diagnosed after the following criteria: definite LE required the histologic evidence of limbic brain inflammation or the detection of antibodies or an underlying malignant tumor. The criteria of possible LE were met if only clinical criteria were fulfilled without detection of an underlying malignancy or positive antibodies. The diagnosis required the exclusion of a viral encephalitis using CSF studies and exclusion of tumor and ischemia.

The distinction between MRI changes in the course of an LE and status epilepticus was performed by assessing the spatial extension of lesions with regard to the affection of limbic, hippocampal, and extrahippocampal tissue typical for LE; the time course (evolution and resolution of diffusion lesions) of limbic affection in relation to disease onset (onset of neurologic symptoms) and absence or presence of status epilepticus in the EEG (electroencephalography); and the presence of bilateral lesions and inflammatory changes such as necrotizing inflammation and hemorrhagic tissue necrosis.[13] Further differentiating clinical criteria were prodromal signs suggestive for encephalitis, time course of clinical recovery, CSF constellation, the presence of epilepsy in the medical history, and the response to antiepileptic therapy in epileptic patients, to steroids and antiviral medication in case of LE.

Transient global amnesia. Fifty-three patients (22 men and 31 women, mean age 64.4 ± 8 years) presenting to our neurological emergency unit and fulfilling established diagnostic criteria of a TGA were studied:[6] (1) the presence of an anterograde amnesia, which was (2) witnessed by an observer, (3) no clouding of consciousness or loss of personal identity, (4) cognitive impairment was limited to amnesia, (5) no focal neurologic or epileptic signs, (6) no history of head trauma or seizures, and (7) resolution of symptoms within 24 hours.

Table 1. Clinical characteristics and cerebrovascular risk factors of patients showing hippocampal damage

	Limbic encephalitis (n = *30*)	*Status epilepticus* (n = *17*)	*Hippocampal ischemia* (n = *50*)	*Transient global amnesia* (n = *53*)	P *value*
Age	60.9 ± 16.6	59.1 ± 21.9	64.2 ± 14.8	64.4 ± 8.2	n.s.
Female sex, *n* (%)	13 (43.3)	11 (64.7)	15 (30.0)	31 (58.5)	n.s.
TIA, *n* (%)	0	0	6 (12.0)	3 (5.7)	n.s.
Arterial hypertension, *n* (%)	14 (46.7)	7 (41.2)	*39 (78.0)*	17 (32.1)	0.000
ICA stenosis, *n* (%)	3 (10.0)	1 (5.9)	*32 (64.0)*	5 (9.4)	0.000
CHD/MI, *n* (%)	2 (6.7)	1 (5.9)	*16 (32.0)*	5 (9.4)	0.003
Atrial fibrillation, *n* (%)	5 (16.7)	1 (5.9)	*17 (34.0)*	5 (9.4)	0.006
Smoking, *n* (%)	2 (6.7)	2 (11.8)	*12 (24.0)*	3 (5.7)	0.029
Cholesterol, *n* (%)	2 (6.6)	3 (17.6)	*17 (34.0)*	7 (13.2)	0.004
Diabetes, *n* (%)	1 (3.3)	3 (17.6)	5 (10.0)	1 (1.9)	n.s.
PAI before, *n* (%)	4 (13.3)	0	11 (22.0)	6 (11.3)	n.s.
Migraine, *n* (%)	1 (3.3)	0	1 (2.0)	*16 (30.2)*	< 0.001

CHD, congestive heart disease; ICA, extracranial section of the internal carotid artery; MI, myocardial infarction; n.s., not significant; PAI, platelet aggregation inhibitor; TIA, transient ischemic attack. Values are given as absolute values and percentage (brackets). Values in italics are significantly different to the other groups' values.

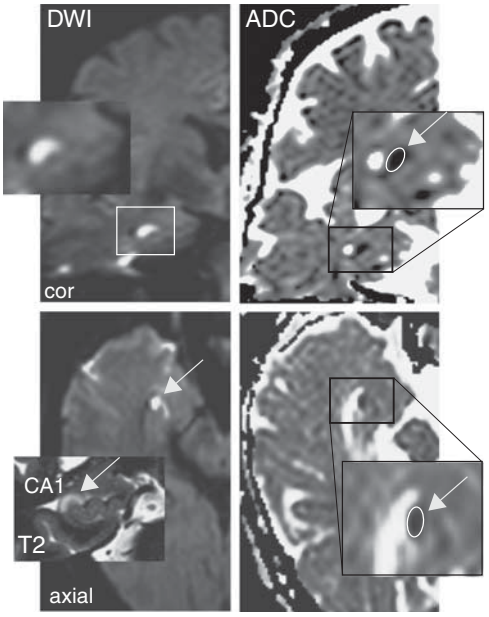

Figure 1. Analysis of diffusion changes and apparent diffusion coefficient (ADC) in the hippocampus. The mean ADC was calculated by manually defining regions of interest (ROIs) that were positioned in the area of the hyperintense DWI lesion in CA1. Magnetic resonance images (3 T) showing a DWI lesion in the head of the right cornu ammonis in the coronal and transversal plane (upper and lower left) with a corresponding lesion in the T2-weighted image (inset, lower left). Inset (upper left) shows the magnified DWI lesion and the ADC signal changes in the coronal (upper right) and transversal plane (lower right) indicating the ROIs for quantifying the ADC values (insets upper and lower right).

Magnetic Resonance Imaging Analysis

Image acquisition and analysis. In all patients a standardized clinical routine MRI (T1- and T2-weighted sequences, DW images) was performed. Magnetic resonance imagings were performed on a 3 T or a 1.5 T unit (Philips Intera Achieva, Philips Healthcare, Eindhoven, The Netherlands). The following sequences were acquired: dual turbo spin echo (TSE) (proton density and T2 weighted): 1.5 T (TR/TE/FA = 2,902/90/90); diffusion-weighted (DWI) echo-planar imaging with subsequent maps of the ADC: 1.5 T (TR/TE/FA = 2,975/84/90), 3T (TR/TE/FA = 3,234/72/90), slice thickness 2 mm; T2-weighted turbo spin echo sequences: 1.5 T (TR/TE/FA = 4,025 /100/90), 3 T (TR/TE/FA = 4,455/100/90); and T1-weighted sequences: 1.5 T TSE (TR/TE/FA = 648/15/70), 3 T gradient echo (TR/TE/FA = 319/2,4/80). The voxel size for the DW images was $1.67 \times 2.12 \times 3$ mm, $0.51 \times 0.65 \times 2$ mm for the T2-weighted images, and $0.4 \times 0.5 \times 5$ mm for T1-weighted images. A high-resolution susceptibility-weighted imaging was included in some patients to detect hemorrhagic tissue changes in HSE.

High resolution MRI (3 T) was performed in 47% of encephalitis patients, in 57% of stroke patients, in 41% of epilepsy patients, and 96% of TGA patients, respectively. The distribution of the different scanners in the stroke, epilepsy, and encephalitis patients was not significantly different across groups, whereas for the TGA group the distribution was significantly different.

Image analysis. All MR images were studied with regard to structural abnormalities of the whole brain including temporal and frontal lobe structures. Only those patients were included who did show abnormalities of the hippocampus or juxtahippocampal region on initial MRI. Only those patients were studied who showed combined and clearly detectable DWI and T2 lesions.

Analysis of diffusion changes and apparent diffusion coefficient in CA1. The mean ADC was calculated by manually defining regions of interest (size 0.05 to 0.15 cm^2) that were positioned in the ADC map corresponding to the area of the hyperintense DWI lesion in CA1 (Figure 1) in the transversal and, if applicable, coronal plane as described.[15] Apparent diffusion coefficient values in the ipsilateral CA1 lesion were compared with the ADC of the contralateral unaffected CA1 area and expressed as ratio of ADC (rADC). The rADC of normal tissue thus corresponds to a value of 1. The rADC was calculated as follows:

$$\text{rADC} = \text{ADC}_{\text{affected}} / \text{ADC}_{\text{healthy}}$$

Analysis was performed by visual inspection of the MR images by two readers experienced in the detection of hippocampal signal abnormalities. Analyzers were masked with regard to the scan time point after onset of disease. Apparent diffusion coefficient parameter maps were calculated using standard software of the MR scanners. Region of interest analysis was performed with postprocessing software on a Philips workstation (ViewForum, Philips Healthcare, The Netherlands). If both hippocampi were affected and did show signal abnormalities, each hippocampus was studied and scored separately and unaffected neocortical tissue regions of interest were used for comparison. Reference ADC values in the neocortex and hippocampus were not significantly different (hippocampus 812 ± 26,913 (± s.e.m.), neocortex 729 ±6; $P > 0.05$). Apparent diffusion coefficient values were plotted in relation to disease onset. The analysis protocol included criteria such as lesion analysis (location, laterality, extension (extrahippocampal), multiplicity of lesions, evidence of chronic tissue change, and long-time course).

Classification of hippocampal lesions. The anatomic classification of hippocampus lesions was based on the classification of Szabo *et al.*[11] According to this classification, four patterns (or types) of hippocampal lesions depending on the extent of the lesion were identified (Figure 2): (a) complete hippocampus; (b) complete lateral hippocampus corresponding to the CA1 area; (c) partial sections of the hippocampus (posterior or anterior, the latter corresponding to the anterior choroidal artery territory); and (d) small focal dot-like lesions confined to the CA1 area. Lesion patterns were mapped with regard to the location within the different sectors of the cornu ammonis (CA-) after Lorento deNo according to the anatomic reference atlas of Duvernoy.

Classification of cerebrovascular risk factors. White-matter hyperintensities were rated according to established MRI criteria:[17] no white-matter hyperintensity (grade 0), punctate (grade 1), early confluent (grade 2), and confluent (grade 3). Lacunar strokes were defined as focal lesions involving the basal ganglia, the internal capsule, the thalamus, or the brain stem not exceeding a maximum diameter of 10 mm and were scored together with clinically silent infarcts.

Other Investigations

Serum and CSF studies included investigations for neurotropic viruses (herpes simplex virus, varicella zoster virus, cytomegalovirus, Epstein–Barr virus, measles virus, and adenovirus) and the study of blood–brain barrier function and immunoglobulin synthesis in the CSF. Serum and CSF from 14 patients included tests for onconeural antibodies such as antibodies against Yo, Ri, Hu, ANNA-3, CV2, MA1+2, gliadin, NMDA, thyreoglobulin, and VGKC (LGI1 and CASPR2).

EEGs were analyzed based on the classification of Lüders and Noachtar classifying a grading of pathology (I to III) based on the assessment of typical EEG criteria such as baseline activity, physiologic, and pathophysiologic patterns (generalized and focal slowing, epileptiform activity). Degree 0 was equivalent to a normal EEG, degree 1 included mild changes in baseline activity, and degree 2 included moderate changes. Notably, degree 3 included severe pathologic changes such as severe generalized or focal slowing of baseline activity and the presence of epileptiform activity.

Statistical Analysis

Statistical analysis was conducted using SPSS 17.0 (SPSS Inc. SPSS Statistics for Windows, Chicago: SPSS Inc.). Parametric tests (Student's *t*-test) or one-way analysis of variance for independent samples were used for parametric measures. Kruskal–Wallis analysis of variance was used for nonparametric measures. Contingency tables for the dichotomous or categorical variables were analyzed by means of the Pearson's chi-square test. Pairwise comparisons were performed to find out differences between groups and time periods. The level of significance was set at 0.05. Values are given as mean ± s.d., unless otherwise stated.

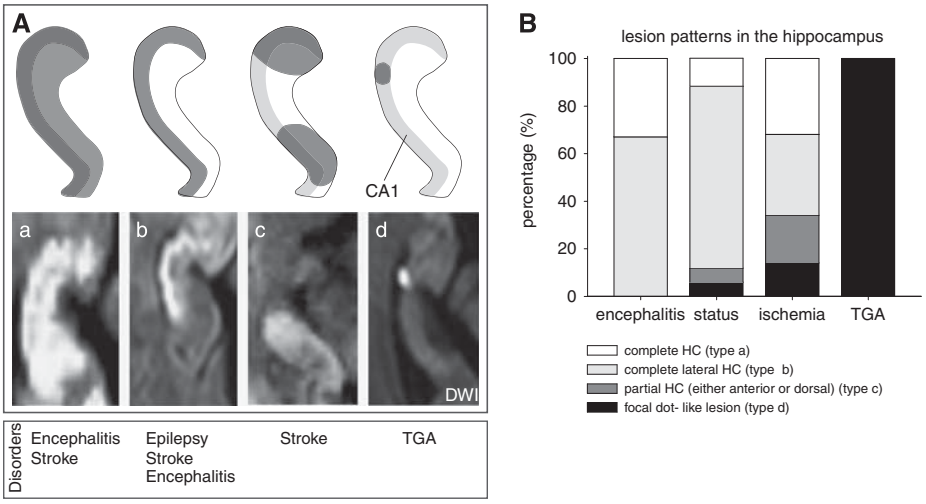

Figure 2. (**A**) Anatomic classification of hippocampal lesions after Szabo *et al*.[11] Four distinct patterns of hippocampal diffusion lesions can be identified depending on the extent of the lesion, including the complete hippocampus (a), the lateral (b) and partial sections of the hippocampus (c; posterior or anterior, the latter corresponding to the anterior choroidal artery), and small, focal dot-like lesions in the lateral hippocampus (d) that correspond to the CA1 area. The lesion pattern of types b and d corresponds to a selective affection of the CA1 region. The distribution of each lesion is presented as a schematic drawing (top row) and as a DWI hyperintense acute lesions (bottom row) on axial orientation. Bottom row indicates the neurologic diseases in which these different spatial lesion patterns can be observed. Only diffusion changes in CA1 were studied. (**B**) Bar graph illustrating the distribution of the different lesion pattern affecting the hippocampus.

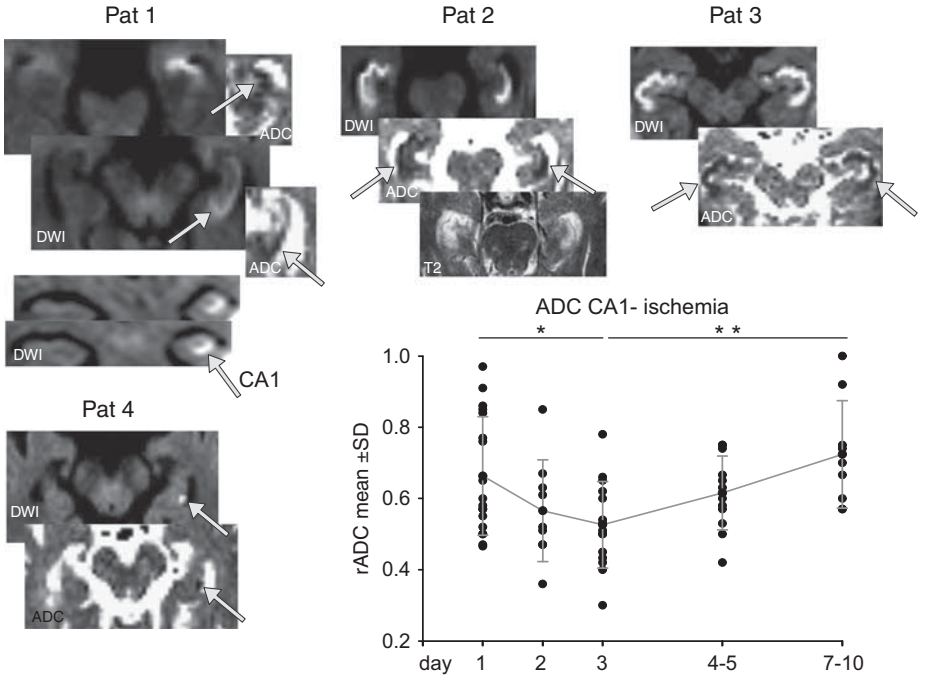

Figure 3. The time course of ischemia-induced diffusion changes indicated by changes in the ratio of apparent diffusion coefficient (rADC) shows a typical minimal reduction around days 2 to 3 with a slow recovery to day 10. Insets show representative DWI images showing a selective affection of the CA1 region including swelling of this region (Pat 1 to 3). Insets show corresponding ADC maps. Pat 4 shows a small dot-like lesion in CA1 after a multiembolic stroke. Notably, Pat 2 shows the affection of the complete bilateral hippocampi with a reduced rADC but with a preferential affection of the CA1 region. Data expressed as mean ± s.d. as well shown as individual values (black dots). *Post hoc* comparisons (*t*-test) of ADC between time periods show that during the acute phase at day 3, ADC was at its minimum and significantly reduced compared with day 1 as well as to the normalization phase after day 7. $^{*}P < 0.05$, $^{**}P < 0.01$. Pat, patient.

RESULTS

Hippocampal Ischemia

Apparent diffusion coefficient measurements in the CA1 field of the cornu ammonis. Fifty patients (35 men and 15 women, mean age 64.2 ± 15 years) were studied presenting with an acute ischemia in the posterior circulation affecting the hippocampus. Within 24 hours after onset and emergence of DWI lesions, rADC values fell below 1.0 (0.66 ± 0.17) and significantly decreased to a minimum rADC of 0.53 ± 0.1 in the 72-hour time window ($P < 0.05$; Figure 3). After day 3, the rADC significantly increased showing mean rADC values of 0.7 within 10 days. The diffusion lesions were accompanied by hyperintense signal changes on T2-weighted images (Figure 3).

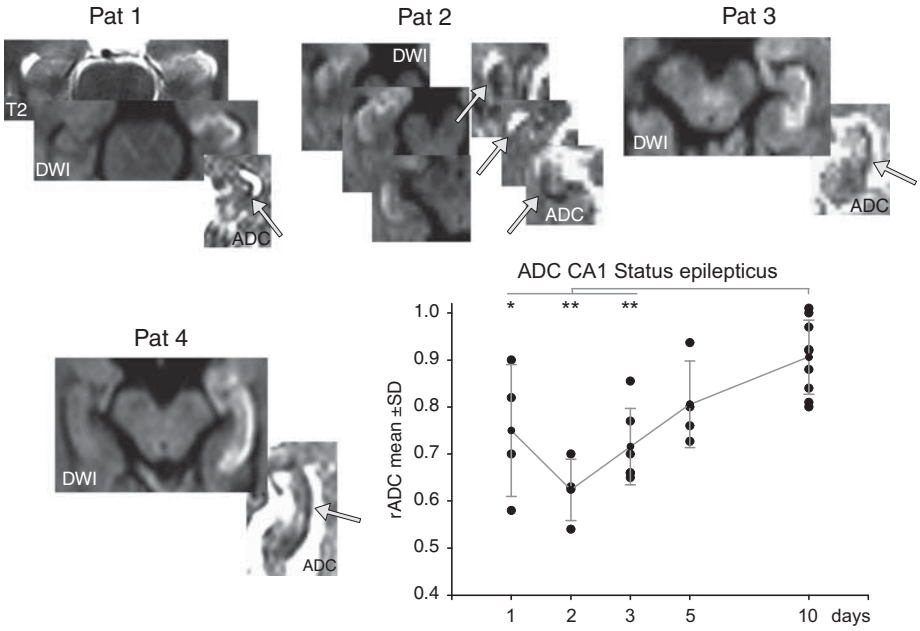

Figure 4. Postictal diffusion changes in the CA1 hippocampal area in patients with a status epilepticus showing a preferential to selective affection of CA1 neurons. Temporal course of the ratio of apparent diffusion coefficient (rADC) changes shows a minimal reduction around days 2 to 3 followed by a normalization to day 10. *Post hoc* comparisons (*t*-test) of ADC between time periods show that during all three time points in the acute phase (days 1 to 3) ADC was significantly reduced compared with the normalization phase around day 10. $*P < 0.05$, $**P < 0.01$.

Patterns of hippocampal lesions. In the majority of patients, multiple diffusion lesions were found outside the hippocampus in the territories of the posterior cerebral artery, posterior inferior cerebellar artery, the superior cerebellar artery, and vertebrobasilar territory whereas only in four patients a pure hippocampal insult was observed. In patients presenting with an ischemic infarction resulting from an occlusion of the posterior cerebral artery, in most cases the head of the hippocampus was less affected than the other parts as a reflection of the supply by the anterior choroidal artery originating from the internal carotidal artery (Figure 2).

One-third (32%) of patients showed lesions involving the complete hippocampus (type a, Figure 3) with an additional involvement of the extrahippocampal posterior cerebral artery territory. Another third (34%) did show selective DWI abnormalities in the lateral part of the hippocampus throughout its entire length correlating to the CA1 region of the cornu ammonis (type b). Twenty percent did show partial infarctions either in the hippocampal head or tail (type c) whereas only 13% ($n = 7$) did show focal lesions in the lateral aspect of the hippocampus body (type d). In patients with a focal lesion, in the majority of cases focal emboli outside the hippocampus were detected. Neurologic symptoms could be attributed to the affection of extrahippocampal structures in most cases and included visual field defects in the majority of patients (68%), paresis and sensory deficits (60%), signs of brain stem affection (14%), and disorders of consciousness including coma (22%). In 16% of patients, routine neurologic examination detected acute amnestic deficits.

Status Epilepticus

Apparent diffusion coefficient measurements in the CA1 field of the cornu ammonis. Seventeen patients (6 men and 11 women, mean age 59.1 ± 22 years) were studied presenting with a status epilepticus or a series of seizures. Naturally, in these patients a higher incidence of pathologic EEGs (III°) could be observed. Within 24 hours after the onset and emergence of DWI lesions rADC values decreased < 1.0 (0.75 ± 0.14) and further declined to a minimum rADC of 0.62 ± 0.06 in the 48-hour time window ($P < 0.05$; Figure 4). After day 3, rADC significantly increased to mean rADC values of 0.9. Again, diffusion lesions were accompanied by hyperintensities on T2-weighted images.

Patterns of hippocampal lesions. In the majority of patients (79%), the hippocampus was affected unilaterally whereas in three patients there was a bilateral affection. Diffusion lesions in epilepsy patients were restricted to the hippocampus. The edema as seen on T2-weighted images was typically less extensive compared with patients with LE. With regard to the patterns of acute diffusion lesions of the hippocampus, the majority of patients (71%) did show a selective affection of the lateral hippocampus (type b) correlating to the CA1 region (Figures 2 and 4). Neurologic symptoms included disorders of consciousness including coma (71%), aphasia (29%), delirium (7%), and amnestic deficits in 50% of patients.

Hippocampal Inflammation

We studied 30 patients (17 men and 13 women, mean age 60.9 ± 17 years) presenting with either a viral or nonviral LE and evidence of an affection of the hippocampus on MRI as well as affection of other limbic/temporomesial structures typical for LE.[13] The majority of patients (70%) did show amnestic deficits, which frequently were unmasked after the recovery from disturbances of consciousness (26%). In some patients, amnestic deficits did show a chronic course. Other neurologic symptoms included aphasia, motor weakness, hemianopia, and accompanying neuropsychiatric symptoms such as disorientation, confusion, and behavioral abnormalities.

By definition, all seven patients with a HSV encephalitis showed a positive HSV PCR in the CSF with a raised cell count and increased protein levels (262 ± 159 cells/μL, protein 640 ± 235 mg/L), whereas patients with a nonviral immune-mediated LE showed a negative HSV PCR in CSF and a lower to normal CSF cell

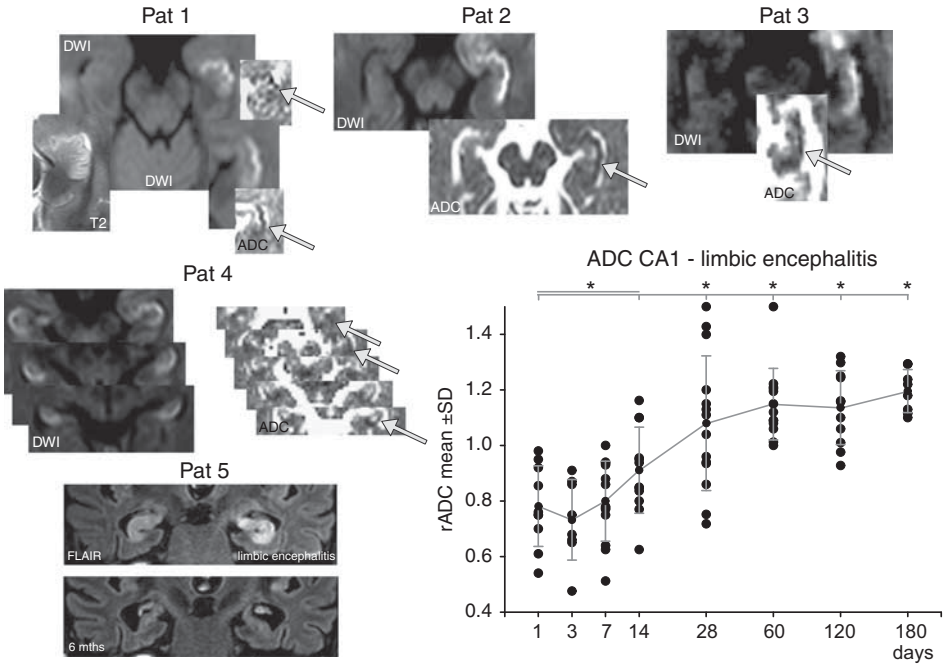

Figure 5. Distribution of DWI lesions in patients with acute limbic encephalitis showing a preferential affection of the lateral hippocampus corresponding to the CA1 region. The time course of the ratio of apparent diffusion coefficient (rADC) in CA1 of the affected hippocampal cornu ammonis shows a reduction from days 1 to 3 and an increase to values >1 after a few weeks. Pairwise comparison shows a significantly different rADC in each of the initial four time points (1 to 14 days) with an increase in the later stages of the disease. Pat 5 shows highly selective involvement of both hippocampi in autoimmune limbic encephalitis (coronal FLAIR) with bilateral swelling and edema. Follow-up imaging 6 months after the encephalitis showed a prominent degeneration and atrophy of both hippocampi, which corresponded to profound memory deficits in this patient as a functional sequel of the hippocampal damage. *Post hoc* comparisons (*t*-test) of ADC between time periods show that during all time points in the acute and subacute phase (days 1 to 14) ADC was significantly reduced compared with the time points in the normalization phase starting around day 28. $^*P < 0.05$. Pat, patient.

count (9.7 ± 31 cells/μL and CSF protein 470 ± 171 mg/L, $P > 0.001$). There were no differences in the time course and the magnitude of CA1 ADC changes between both groups. Tests for onconeural antibodies were positive in three patients (LGI1, $n = 2$; NMDA-AB, $n = 1$). Investigations for an underlying primary malignancy were positive in four patients with negative antibodies, so that patients were defined as having a possible paraneoplastic LE. This classification of an LE was corroborated by the time course of their MRI findings.

Apparent diffusion coefficient measurements in the CA1 field of the cornu ammonis. Early after disease onset, rADC values fell below 1.0 (0.78 ± 0.15) and further declined to a minimum rADC of 0.73 ± 0.1 in the 72-hour time window (Figure 5). Pairwise comparison shows a significantly different rADC of each of the initial four time points (1 to 14 days) with the later stages of the disease. Probably because of the slower time course of the infectious and inflammatory processes, rADC values did show a protracted time course. Within four weeks, the rADC significantly increased to values ~1.0 and in due course within the follow-up period up to 120 days further elevated to values >1.0. Lesions in DW imaging were accompanied by hyperintensities on T2-weighted images (Figure 5). This time course correlated to a state-dependent progression from an initial diffusion lesion with ADC reductions and T2 prolongation as a reflection of a CA1 cytotoxic edema with hippocampal swelling into increased ADC values and decrease of hippocampal edema. Thirteen patients with encephalitis did show an atrophy of the affected hippocampus in due course.

Patterns of hippocampal lesions. In 26 patients only one hippocampus was affected whereas in four patients there was a bilateral affection. Multiple diffusion lesions outside the hippocampus were found in the majority of patients not only involving the adjacent medial temporal lobe but also the amygdala, hypothalamus, insular, and cingulate cortices. In patients with HSE, the extrahippocampal affection was considerably more extensive than in patients with non-HSE or in patients with status epilepticus. In the majority of patients, either the lateral hippocampus (67%, type c) or the complete hippocampus (33%) with a predominant involvement of the CA1 region was affected, however, with additional juxtahippocampal lesions (Figures 2 and 5).

Transient Global Amnesia

Apparent diffusion coefficient measurements in the CA1 field of the cornu ammonis. Within 24 hours after onset of TGA, rADC values were below 1.0 (0.76 ± 0.15) and further progressed to a minimum of 0.69 ± 0.1 in the 48-hour time window ($P < 0{,}05$; Figure 6). After 72 hours, the rADC increased showing mean rADC values of 0.82 within the observation period of 5 days. Focal DWI lesions in the hippocampus were accompanied by hyperintensities on T2-weighted images (Figure 6).

Patterns of hippocampal lesions. In all patients, typical focal dot-like TGA lesions (type d) were found in the lateral region (CA1) of the cornu ammonis without evidence of further diffusion lesions outside the hippocampus (Figure 6) or more extensive lesions. Clinically, patients in the acute phase did show a profound impairment of their episodic memory with an anterograde and retrograde amnesia. Retention span lasted just a few minutes while the retrograde amnesia extended years into the past. The amnestic syndrome lasted <24 hours. Analysis of cerebrovascular risk factors

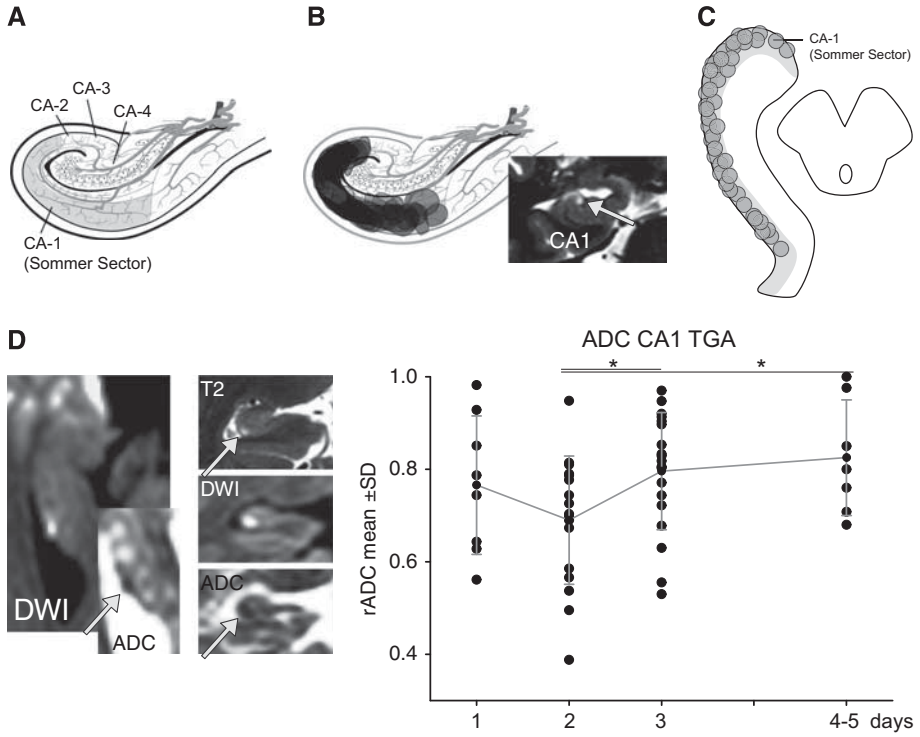

Figure 6. Diffusion lesions detectable in patients with a transient global amnesia (TGA). (**A**) An anatomic template showing the various subfields of the hippocampal cornu ammonis according to Lorente de No. (**B**) The distribution of the DWI/T2 lesions within the cornu ammonis show that the lesions are confined to the CA1 subfield. (**C**) A model of the hippocampus in axial orientation showing the anterior–posterior distribution of the magnetic resonance imaging (MRI) lesions in TGA. (**D**) A representative 3 T MRI in a patient with TGA, showing the typical lesion in the diffusion-weighted imaging and apparent diffusion coefficient (ADC) map and the corresponding lesions in the T2-weighted images. *Post hoc* comparisons (*t*-test) of ADC between time periods indicate a significant increase in ADC from day 2 to days 4 to 5. $^*P < 0.05$.

did show an increased prevalence of arterial hypertension and migraine in the patients' medical history (Table 1).

Comparison Between Groups

In all patients, MRI analysis showed that the CA1 sector of the hippocampus was always affected in a sense that a hippocampal affection without involvement of CA1 could not be observed. In patients with an affection of the complete hippocampus, such as in LE, CA1 region was predominantly involved where signal alterations were most prominent (Figure 5). A comparison of the rADC CA1 did show a significant lower minimum rADC in patients with a hippocampal ischemia (0.52 ± 0.1, $P < 0.05$) compared with encephalitis (0.73 ± 0.1), status epilepticus (0.62 ± 0.3), or TGA (0.69 ± 0.1) suggesting that an hypoxic–ischemic insult results in a stronger impairment of cellular metabolism with subsequent restriction of water diffusion. Apart from patients with TGA, which all received a 3 T MRI, there was no significant difference in the minimum rADC between 3 T and 1.5 T scanners in stroke (0.48 ± 0.1 (3 T) versus 0.55 ± 0.12 (1.5 T)), encephalitis (0.73 ± 0.12 (3 T) versus 0.74 ± 0.2 (1.5 T)), and status epilepticus (0.66 ± 0.05 (3 T) versus 0.59 ± 0.06 (1.5 T; ± s.d.)).

With regard to the spatial lesion pattern of the hippocampus, TGA patients showed the most selective distribution of hippocampal lesions as only focal lesions in CA1 could be observed. A minority of stroke patients did also show similar lesions as a consequence of embolism but these patients also exhibited extrahippocampal focal lesions that could not be detected in TGA. Encephalitis and epilepsy patients did show a preferential affection of the CA1 sector on its entire rostral–dorsal axis (type b), while the pattern in hippocampal infarction was mixed depending on the nature of the stroke etiology and affected vascular territory. As shown in Table 1, patients with a hippocampal ischemia did show a higher prevalence of cerebrovascular risk factors whereas patients with a TGA did show a higher prevalence of a history of migraine as reported earlier.[18] With regard to the distribution and frequency of markers of cerebral small–vessel disease, patients with a hippocampal infarction did show an increased lesion load with regard to punctuate or confluent white-matter hyperintensities and preexisting infarcts. The increased cerebrovascular risk profile in stroke patients was reflected in a higher lacunar lesion load.

DISCUSSION

The regional vulnerability of the hippocampus to acute injury with its susceptibility of the CA1 field has been recognized for more than a century and patients with hippocampal infarctions often present with memory disturbances. In the last 30 years, critical pathophysiologic processes have been extensively studied in animal models and cellular mechanism of this vulnerability is a subject of intense research.[5] Here, we show in humans that hippocampal CA1 neurons are selectively impaired by acute injury in neurologic disorders and that the impairment follows the typical time course seen in animal models of delayed neuronal death with a maximum impairment 48 to 72 hours after the insult. However, hippocampal damage displays an uniform time course irrespective of the nature of the insult. The degree of diffusion changes in the CA1 region of the hippocampus correlates to the magnitude of the insult and mirrors the degree of cellular metabolic impairment. Further, acute neurologic insults display

differential spatial pattern of hippocampal damage that could be used for discriminating the underlying pathology.

Since the first systematic descriptions of the vulnerability of the CA1 region in the gerbil[3] and rat[4] showing a time course with a 'delayed neuronal death' of CA1 neurons 48 to 72 hours after the insult, the cellular responses in transient ischemia has been the most widely used model since then.[1] In recent years, *in vivo* MRI in mice and rats has been increasingly used to further dissect the cellular mechanisms and to provide translational models for human disease. The development of postischemic hippocampal lesions was studied by measuring the time course of the ADC in rats and gerbils using MRI. The ADC decreased from day 1 to day 4 in CA1, which was accompanied by considerable glial cell proliferation, marked neuronal cell death, and developing reactive gliosis.[10,19,20] The decrease of the ADC paralleled a decreased volume fraction of the extracellular space and an increased tortuosity.[10] Seven days after reperfusion, the ADC in CA1 renormalized to control values or even above, a phenomenon that can be seen also in human CA1. It has been suggested that renormalization of the ADC in the CA1 region in rats is the result of extensive neuronal cell death as the number of neurons is decreased by 75%, however, other factors such as neuronal shrinkage because of apoptosis and increased tortuosity because of astrogliosis may contribute.[10] Histopathologic studies of structural changes in hippocampal neurons after ischemia show that ischemic damage results in cellular swelling that includes mitochondrial swelling and subsequent disintegration.[21] This leads to further decreases in protein synthesis, protease-dependent degeneration, and apoptosis. It has also been suggested that distinct populations of hippocampal cells in CA1, CA3, and dentate gyrus are differentially vulnerable to ischemia, as hippocampal interneurons are believed to be more resistant to the effects of ischemia than larger projection neurons.[22,23]

In the final pathway of this regional vulnerability in CA1 pyramidal cells, excess glutamate release, and stimulation of postsynaptic glutamatergic receptors including NMDA receptors have been widely considered a key mechanism in CA1 neuronal death.[1,24–26] CA1 neurons express a considerably higher density of NMDA NR2 subunits than do CA3 or dentate gyrus neurons.[25] Acute ischemia leads to energy depletion because of a loss of oxygen and glucose with subsequent impaired generation of ATP, increased membrane permeability and the facilitated production of reactive oxygen species.[27] As a consequence of altered ATP supplies, changes in ion gradients lead to the accumulation of extracellular glutamate, and the resulting intracellular accumulation of Ca^{2+} results in cytotoxicity.[28] Oxidative stress is the result of an imbalance between the generation of deleterious reactive oxygen and nitrogen species and the cell's compensatory mechanisms.[28] The differential regional vulnerability of cerebral structures is at least partly also a reflection of regional differences in antioxidant enzymes.[5,29]

A common finding in these cases is the unilateral or bilateral involvement of the hippocampus. Hippocampal strokes can be classified with regard to their anatomic distribution, which is a reflection of the type of insult as well as the vascular arrangement.[11]

Postictal Changes in the Hippocampus

Neuroimaging data show that CA1 can be selectively affected in post and periictal states.[14] It is thought that this cytotoxic component may reflect the consequences of intrinsic glutamate–mediated seizure activity rather than the effects of hypoxia or cerebral ischemia. In rats with kainate-induced seizures, MRI shows a decrease in the ADC of the limbic and hippocampal structures within the first 72 hours.[30] In patients with complex partial status epilepticus, a decrease in the ADC within the epileptogenic hippocampal zones and subcortical areas of propagation has been observed within 3 days of seizure onset. A transient reduction in the ADC in CA1 and a corresponding lactate peak in the MR spectroscopy was described in 12 patients within 48 hours of acute symptomatic seizures or status epilepticus, whereas interictally the ADC in the hippocampus was increased.[14] The magnitude of neuronal impairment and thus subsequent diffusion changes is dependent on the duration of the seizure activity and concomitant metabolic need.[31]

The time course of periictal restricted diffusion in epilepsy can be divided into different stages.[32,33] During both acute and active seizures, the metabolic demands of the affected cells increase dramatically and lead to an increase in cerebral blood flow without concomitant changes in the ADC. The subacute yet active stage is characterized by vasogenic extracellular edema with a concomitant increase in the ADC, although various studies have not been able to detect this stage.[34] Frequently, however, complex changes in the ADC over time—such as decreases, generalized changes, and increases in the ADC—can be observed in the hippocampus from 2 to 210 minutes after a seizure, depending on the type of seizure and the latency period between the seizure and scanning.[8] There are limited data describing the time course of postictal ADC changes.[35] Ictal or periictal increases in the ADC are likely a reflection of vasogenic extracellular edema in the hippocampus.[33] This periictal stage is typically followed by a postictal stage with a decrease in the ADC that parallels that of cytotoxic intracellular edema and lasts 1 to 3 days, which might be the result of transient hyperperfusion.[36]

Hippocampal Inflammation

In inflammatory processes such as HSE and LE, MRI reveals a predilection for limbic structures (e.g., the hippocampus, amygdala, hypothalamus and insular and cingulate cortices), but the hippocampus is often predominantly affected (Figure 2).[37] Hyperintense DWI abnormalities in the hippocampus have been reported in the initial stages of the disease and are accompanied by a reduction in the ADC that is likely the result of cytotoxic edema.[38] Serial MRIs in patients with HSE have revealed a reduction in the ADC in neocortical tissue within the first 5 to 6 days after the onset of the disease. Increased ADC values have also been reported, which likely reflects combined vasogenic and extracellular edema.[12] Both of these stages seem to correlate with a progression from cytotoxic edema to inflammatory vasogenic edema in due course, with the latter reflecting increased permeability of the blood–brain barrier over the course of the immune response to the infection.

In LE, the temporal time course of MRI changes has been studied in detail by Urbach *et al.*[13] The hippocampi including CA1 showed prominent swelling in the T2-weighted imaging and FLAIR typically seen within the first 3 months of disease onset. Again, the progression of the reduced ADC toward elevated values in the early stages of the disease suggests a dynamic course of the diffusivity from cytotoxic edema to a vasogenic edema. Typically, atrophic temporal mesial or hippocampal structures were observed in the later stages.

Transient Global Amnesia

Recent data using high-resolution MRI in TGA have shown that focal hyperintense lesions in the hippocampus are restricted to the CA1 region (Figure 6).[15,39] The temporal evolution of hippocampal lesions has been studied by measuring the time course of the ADC of hippocampal DWI lesions in TGA patients using serial 3 T MRI.[15] DWI lesions evolve after 24 to 48 hours and are detectable up to 7 to 10 days after the TGA episode. Correspondingly, the ADC values are at a minimum between 24 to 72 hours and return to normal around day 10.[15] Complementary imaging studies combining MRI and focal MR spectroscopy of CA1 have revealed a distinct lactate peak suggesting the presence of acute metabolic stress in the CA1 neurons during a TGA episode.[39]

Cellular Pathways of Hippocampal Damage

Although the final pathways in noxious insults to hippocampus, such as ischemia, hypoglycemia, and status epilepticus, may all lead to neuronal hippocampal damage and necrosis, it has been suggested that these clinical conditions may have different initial pathophysiologic cascades.[40] During ischemia, for example, the cellular metabolic rate rapidly and dramatically declines, which profoundly impairs ion homeostasis and cellular redox systems and rapidly causes acidosis. In hypoglycemia, cellular oxygen consumption continues, with a loss of high-energy phosphates and ion homeostasis, whereas redox systems become oxidized and acidosis is severely reduced. During seizure activity, the cellular metabolic rate increases, although the cellular energy state and ion homeostasis are largely preserved. This preservation suggests that necrosis of hippocampal cells occurs despite sufficient oxygenation and might not be strictly related to energy failure.[40]

Our data comparing different neurologic disorders show a rather uniform time course of the development of diffusion lesion in CA1, thus suggesting that the final pathophysiologic cascade is independent of the nature of the impact on CA1 neurons. The data from human, animal, and experimental studies fits well with the degree and time course of the ADC than can be observed in our patients. Interestingly, ischemia-induced changes in the CA1 sector results in a significantly pronounced diffusion lesion compared with epilepsy-, encephalitis-, and TGA-induced changes, suggesting that the hypoxic–ischemic insult results in a stronger impairment of cellular metabolism leading to a more severe restriction of water diffusion. Thus, the diffusion changes observed in CA1 are a phase-dependent reflection of the underlying pathologic changes. The acute phase is characterized by a cytotoxic edema with subsequent restricted diffusion and decreased ADC followed by a subacute stage with predominantly vasogenic edema and normalizing or increasing ADC. The chronic phase shows elevated ADC values indicating vasogenic edema or gliosis.

In chronic diseases, however, such as in neurodegenerative diseases, chronic epilepsy, or neuropsychiatric disorders in which the time course and type of pathologic changes is much slower, the regional vulnerability might preferentially affect other hippocampal structures such as the dentate gyrus or the CA3 area. This might lead to a differential impairment of hippocampal subnetworks and its functions depending on the nature of the pathological process.[41]

In conclusion, MRI in humans offers valuable insight into the cellular responses to noxious influences on the hippocampus, and future research should focus on translational aspects combining state-of-the-art high-resolution imaging and experimental imaging methods to further dissect pathophysiologic cellular changes in neurologic disease affecting the hippocampus.

AUTHOR CONTRIBUTIONS

Research project conception, organization, and execution; statistical analysis execution; writing the first draft, review, and critique: TB; statistical analysis design, execution, review, and critique: JD; research project execution; manuscript review and critique: SR, CF, AR, and HB; statistical analysis review and critique; manuscript review and critique: GD and OJ.

DISCLOSURE/CONFLICT OF INTEREST

The authors declare no conflict of interest.

REFERENCES

1 Schmidt-Kastner R, Freund TF. Selective vulnerability of the hippocampus in brain ischemia. *Neuroscience* 1991; **40**: 599–636.
2 Kirino T. Delayed neuronal death. *Neuropathology* 2000; **20**: S95–S97.
3 Kirino T. Delayed neuronal death in the gerbil hippocampus following ischemia. *Brain Res* 1982; **239**: 57–69.
4 Pulsinelli WA, Brierley JB, Plum F. Temporal profile of neuronal damage in a model of transient forebrain ischemia. *Ann Neurol* 1982; **11**: 491–498.
5 Wang X, Michaelis EK. Selective neuronal vulnerability to oxidative stress in the brain. *Front Aging Neurosci* 2010; **2**: 12.
6 Bartsch T, Schonfeld R, Muller FJ, Alfke K, Leplow B, Aldenhoff J *et al.* Focal lesions of human hippocampal CA1 neurons in transient global amnesia impair place memory. *Science* 2010; **328**: 1412–1415.
7 Kadar T, Dachir S, Shukitt-Hale B, Levy A. Sub-regional hippocampal vulnerability in various animal models leading to cognitive dysfunction. *J Neural Transm* 1998; **105**: 987–1004.
8 Forster A, Griebe M, Gass A, Kern R, Hennerici MG, Szabo K. Diffusion-weighted imaging for the differential diagnosis of disorders affecting the hippocampus. *Cerebrovasc Dis* 2012; **33**: 104–115.
9 Szabo K, Forster A, Gass A. Conventional and diffusion-weighted MRI of the hippocampus. *Front Neurol Neurosci* 2014; **34**: 71–84.
10 Anderova M, Vorisek I, Pivonkova H, Benesova J, Vargova L, Cicanic M *et al.* Cell death/proliferation and alterations in glial morphology contribute to changes in diffusivity in the rat hippocampus after hypoxia-ischemia. *J Cereb Blood Flow Metab* 2010; **31**: 894–907.
11 Szabo K, Forster A, Jager T, Kern R, Griebe M, Hennerici MG *et al.* Hippocampal lesion patterns in acute posterior cerebral artery stroke: clinical and MRI findings. *Stroke* 2009; **40**: 2042–2045.
12 Hatipoglu HG, Sakman B, Yuksel E. Magnetic resonance and diffusion-weighted imaging findings of herpes simplex encephalitis. *Herpes* 2008; **15**: 13–17.
13 Urbach H, Soeder BM, Jeub M, Klockgether T, Meyer B, Bien CG. Serial MRI of limbic encephalitis. *Neuroradiology* 2006; **48**: 380–386.
14 Parmar H, Lim SH, Tan NC, Lim CC. Acute symptomatic seizures and hippocampus damage: DWI and MRS findings. *Neurology* 2006; **66**: 1732–1735.
15 Bartsch T, Alfke K, Deuschl G, Jansen O. Evolution of hippocampal CA-1 diffusion lesions in transient global amnesia. *Ann Neurol* 2007; **62**: 475–480.
16 Bartsch T, Döhring J, Brauer H, Lagies J, Rohr A, Deuschl G *et al.* Selective neuronal vulnerability of hippocampal CA1 neurons in acute neurological disorders. *Neuroscience 2013*. Society for Neuroscience: San Diego, USA, 2013.
17 Enzinger C, Thimary F, Kapeller P, Ropele S, Schmidt R, Ebner F *et al.* Transient global amnesia: diffusion-weighted imaging lesions and cerebrovascular disease. *Stroke* 2008; **39**: 2219–2225.
18 Bartsch T, Deuschl G. Transient global amnesia: functional anatomy and clinical implications. *Lancet Neurol* 2010; **9**: 205–214.
19 Zhu L, Saito N, Abe O, Okubo T, Yamada H, Kawahara N *et al.* Changes in the apparent diffusion coefficient of water and T2 relaxation time in gerbil hippocampus after mild ischemia. *Neuroreport* 2000; **11**: 3333–3336.
20 Shepherd TM, Thelwall PE, Blackband SJ, Pike BR, Hayes RL, Wirth ED 3rd. Diffusion magnetic resonance imaging study of a rat hippocampal slice model for acute brain injury. *J Cereb Blood Flow Metab* 2003; **23**: 1461–1470.
21 Nikonenko AG, Radenovic L, Andjus PR, Skibo GG. Structural features of ischemic damage in the hippocampus. *Anat Rec* 2009; **292**: 1914–1921.
22 Harry GJ, Lefebvre d'Hellencourt C. Dentate gyrus: alterations that occur with hippocampal injury. *Neurotoxicology* 2003; **24**: 343–356.
23 Avignone E, Frenguelli BG, Irving AJ. Differential responses to NMDA receptor activation in rat hippocampal interneurons and pyramidal cells may underlie enhanced pyramidal cell vulnerability. *Eur J Neurosci* 2005; **22**: 3077–3090.
24 Bonde C, Noraberg J, Noer H, Zimmer J. Ionotropic glutamate receptors and glutamate transporters are involved in necrotic neuronal cell death induced by oxygen-glucose deprivation of hippocampal slice cultures. *Neuroscience* 2005; **136**: 779–794.
25 Butler TR, Self RL, Smith KJ, Sharrett-Field LJ, Berry JN, Littleton JM *et al.* Selective vulnerability of hippocampal cornu ammonis 1 pyramidal cells to excitotoxic insult is associated with the expression of polyamine-sensitive N-methyl-D-asparate-type glutamate receptors. *Neuroscience* 2010; **165**: 525–534.
26 Lalonde CC, Mielke JG. Selective vulnerability of hippocampal sub-fields to oxygen-glucose deprivation is a function of animal age. *Brain Res* 2014; **1543**: 271–279.
27 Wang X, Pal R, Chen XW, Limpeanchob N, Kumar KN, Michaelis EK. High intrinsic oxidative stress may underlie selective vulnerability of the hippocampal CA1 region. *Brain Res Mol Brain Res* 2005; **140**: 120–126.
28 Bao X, Pal R, Hascup KN, Wang Y, Wang WT, Xu W *et al.* Transgenic expression of Glud1 (glutamate dehydrogenase 1) in neurons: in vivo model of enhanced glutamate release, altered synaptic plasticity, and selective neuronal vulnerability. *J Neurosci* 2009; **29**: 13929–13944.
29 Wang X, Zaidi A, Pal R, Garrett AS, Braceras R, Chen XW *et al.* Genomic and biochemical approaches in the discovery of mechanisms for selective neuronal vulnerability to oxidative stress. *BMC Neurosci* 2009; **10**: 12.

30 Engelhorn T, Weise J, Hammen T, Bluemcke I, Hufnagel A, Doerfler A. Early diffusion-weighted MRI predicts regional neuronal damage in generalized status epilepticus in rats treated with diazepam. *Neurosci Lett* 2007; **417**: 275–280.
31 Fujikawa DG. The temporal evolution of neuronal damage from pilocarpine-induced status epilepticus. *Brain Res* 1996; **725**: 11–22.
32 Wieshmann UC, Symms MR, Shorvon SD. Diffusion changes in status epilepticus. *Lancet* 1997; **350**: 493–494.
33 Yu JT, Tan L. Diffusion-weighted magnetic resonance imaging demonstrates parenchymal pathophysiological changes in epilepsy. *Brain Res Rev* 2008; **59**: 34–41.
34 Wall CJ, Kendall EJ, Obenaus A. Rapid alterations in diffusion-weighted images with anatomic correlates in a rodent model of status epilepticus. *AJNR Am J Neuroradiol* 2000; **21**: 1841–1852.
35 Di Bonaventura C, Bonini F, Fattouch J, Mari F, Petrucci S, Carni M *et al.* Diffusion-weighted magnetic resonance imaging in patients with partial status epilepticus. *Epilepsia* 2009; **50**: 45–52.
36 Gong G, Shi F, Concha L, Beaulieu C, Gross DW. Insights into the sequence of structural consequences of convulsive status epilepticus: a longitudinal MRI study. *Epilepsia* 2008; **49**: 1941–1945.
37 Finke C, Kopp UA, Scheel M, Pech LM, Soemmer C, Schlichting J *et al.* Functional and structural brain changes in anti-N-methyl-D-aspartate receptor encephalitis. *Ann Neurol* 2013; **74**: 284–296.
38 McCabe K, Tyler K, Tanabe J. Diffusion-weighted MRI abnormalities as a clue to the diagnosis of herpes simplex encephalitis. *Neurology* 2003; **61**: 1015–1016.
39 Bartsch T, Alfke K, Wolff S, Rohr A, Jansen O, Deuschl G. Focal MR spectroscopy of hippocampal CA-1 lesions in transient global amnesia. *Neurology* 2008; **70**: 1030–1035.
40 Siesjo BK, Wieloch T. Epileptic brain damage: pathophysiology and neurochemical pathology. *Adv Neurol* 1986; **44**: 813–847.
41 Small SA, Schobel SA, Buxton RB, Witter MP, Barnes CA. A pathophysiological framework of hippocampal dysfunction in ageing and disease. *Nat Rev Neurosci* 2011; **12**: 585–601.